NREL/TP-442-6930 • UC Category: 1213 • DE95004049

Conf-9506145--2

Advanced System Identification Techniques for Wind Turbine Structures

Jan T. Bialasiewicz and Richard M. Osgood

Prepared for
1995 SEM Spring Conference
Grand Rapids, Michigan
June 12-14, 1995

National Renewable Energy Laboratory
1617 Cole Boulevard
Golden, Colorado 80401-3393
A national laboratory of the U.S. Department of Energy
Managed by Midwest Research Institute
for the U.S. Department of Energy
under contract No. DE-AC36-83CH10093

Prepared under Task No. WE518210

March 1995

NOTICE

Available to DOE and DOE contractors from:
Office of Scientific and Technical Information (OSTI)
P.O. Box 62
Oak Ridge, TN 37831
Prices available by calling (615) 576-8401

Available to the public from:
National Technical Information Service (NTIS)
U.S. Department of Commerce
5285 Port Royal Road
Springfield, VA 22161
(703) 487-4650

Printed on paper containing at least 50% wastepaper and 10% postconsumer waste

ADVANCED SYSTEM IDENTIFICATION TECHNIQUES FOR WIND TURBINE STRUCTURES

Jan T. Bialasiewicz
Richard M. Osgood

National Renewable Energy Laboratory
National Wind Technology Center
1617 Cole Boulevard
Golden, CO 80401-3393

ABSTRACT
The new approach to modal parameter identification, presented in this paper, uses an asymptotically stable observer to form a discrete state-space model for a wind turbine structure. The identification is performed using input-output time-series. A special software package developed in this research has been tested using the data generated by the ADAMS®[1] model of the Micon 65/13 wind turbine structure. Numerical and graphical presentation of some of the results, generated by the programs developed, illustrates the range of their applicability.

1 INTRODUCTION

The goal of this research was to develop advanced system identification techniques to accurately measure the frequency response functions of a wind turbine structure immersed in wind noise. To allow for accurate identification, we developed a special test signal called the **P**seudo-**R**andom **B**inary **S**equence (PRBS). The PRBS signal produces the wide-band excitation necessary to perform system identification in the presence of wind noise. The techniques presented here will enable researchers to obtain modal parameters from an operating wind turbine. More importantly, the algorithms we have developed and tested (so far using input-output data from an ADAMS model of a wind turbine structure) permit state-space representation of the system under test, particularly the modal state-space representation. This is the only system description that reveals the internal behavior of the system, such as the interaction between the physical parameters, and which, in contrast to transfer functions, is valid for non-zero initial conditions.

Sandia National Laboratories' (SNL) Natural Excitation Technique (NExT) for modal parameter extraction from operating wind turbines uses the measured system outputs obtained as a result of natural wind excitation [2]. Generally, the cross-correlation function of such outputs has the shape of the system's impulse response and therefore allows one to extract modal frequencies and damping ratios. SNL's researchers have done this using one of the system realization algorithms (such as the Eigensystem Realization Algorithm developed at the National Aeronautical and Space Administration's [NASA] Langley Research Center). In other words, SNL researchers assume that the cross-correlation function represents the sequence of Markov parameters or impulse response of the system to be identified. Such an assumption will not lead to any input-output model of the system, such as a transfer function or state-space representation. To identify any of these input-output characteristics, it is not enough to excite the system with a frequency-rich signal (such as natural wind noise) but one must also measure this signal. System identification requires a frequency-rich input-output history.

Researchers have developed many system identification techniques and applied them to state-space models to identify modal parameters. Most techniques use sampled-impulse system response histories, known as system Markov parameters. The new approach, presented here, uses the results obtained by researchers at NASA's Langley Research Center [3-5]. Rather than identifying the system Markov parameters (which may exhibit very slow decay), one can use an asymptotically stable observer to form a stable, discrete state-space model to identify the system.

The organization of this paper is as follows. In Section 2, we discuss how the excitation or input signal should be chosen. Then, in Section 3, we present the problem of making a proper selection of measurements to be obtained from a modal test. In Section 4, we introduce the Observer/Kalman Filter state-space model whose identification is performed by the

[1] ADAMS is a registered trademark of Mechenical Dynamics, Inc.

MATLAB®[2] program **flokuy.m**, originally introduced in [1]. Finally, in Section 5, we present general information on the identification methodology. Additional details are discussed in the Appendix, where a case study is presented using input-output time-series obtained from the ADAMS model of the wind turbine Micon 65/13. Section 6 concludes the paper and summarizes the results presented.

2 SELECTION OF INPUT SIGNAL

Both the simulation and the experiment provide sampled input-output data. The sampling interval T has to be properly chosen. The Nyquist frequency

$$\omega_N = \frac{\pi}{T} \text{ [rad / s]} \quad \text{or} \quad f_N = \frac{1}{2T} \text{ [Hz]} \qquad (1)$$

must be greater than the bandwidth of interest $f_{\max}$ of the structure. If the structure bandwidth considered is limited by the frequency $f_{\max}$, then (according to the sampling theorem) discrete-time representation of this process requires a sampling frequency of $f_S > 2f_{\max}$. The rule of thumb is to choose $f_s = (6 \text{ to } 25) f_{\max}$ with $f_s = 1/T$ as high as possible. On the other hand, in order to correctly identify the steady-state gain of the process, the duration of at least one of the pulses in the PRBS must be greater than the rise time t_R of the process.

The value of the input PRBS signal can switch between two levels every T_{prbs} seconds. In other words, T_{prbs} is the switching period. As explained in [8], the spectrum of the pseudo-random binary signal approximates the broad-band noise, provided its clock frequency is fast enough and its sequence length is large enough. The PRBSs are generated by shift registers with feedback (implemented in hardware or software). The maximum length L of a sequence is

$$L = 2^N - 1 \qquad (2)$$

where N is the number of stages of the shift register. As mentioned earlier, the maximum duration of at least one pulse, NT_{prbs}, must exceed the rise time of the process:

$$NT_{prbs} > t_R \qquad (3)$$

The clock frequency f_{prbs} for the PRBS must accordingly be chosen as a submultiple of the sampling frequency f_S. If $f_{prbs} = f_S / p$ (p=1,2,...), then $T_{prbs} = T\,p$ and, combining this with the inequality (3), we obtain the following condition that must be fulfilled:

$$N > \frac{t_R}{T\,p} = \frac{t_R}{T_{prbs}} \qquad (4)$$

Because lowering the clock frequency of the PRBS will reduce the frequency range in which its spectral density can be considered constant, choosing $p \le 4$ is recommended [7].

Suppose that the process to be identified has the bandwidth of 5 Hz but at the same time the bandwidth of interest is much higher. The time constant of such a process is approximately equal to 0.2 s and the rise time is approximately 0.4 s. If we set N=10, then in view of equation (3) we should have $T_{prbs} = pT > 0.04$. Because we want the sampling interval to be as small as practical, we shall choose p=4 and T=0.01. This results in Nyquist frequency f_N =50 Hz, and we can expect accurate identification of the modal frequencies lower than 10 Hz. Higher modal frequencies will be identified with some distortions. If the required bandwidth of interest is 30 Hz, then, for accurate identification, the sampling frequency should at least be 180 Hz or the sampling period should be approximately 0.005 s that gives f_N=100 Hz. On the other hand, assuming that the PRBS input sequence is generated with N=10 and p=4 (4092 samples long), the maximum duration of a pulse in the input signal is pNT=0.2 s. Such an input sequence will not properly excite low frequency modes, resulting in considerable distortions in the low-frequency range of the identified frequency response. A practical solution is to run several experiments with different sampling intervals and to obtain for each of them the frequency response accurate in a particular frequency range.

3 SELECTION OF MEASUREMENTS

The problem of the proper selection of measurements has been studied using simulation data for the ADAMS analytical model of the Micon 65/13 wind turbine structure. There were 32 measurement points along the structure but at each of them we had two virtual accelerometers measuring in two directions: Y and Z, according to the local coordinate systems, different for each blade and the tower.

To excite all the modes, the simulation was performed for three out-of-plane excitations and one in-plane excitation, all of the same PRBS type. The out-of-plane excitations were two near the blade tips and one at 2/3 of the tower height. For each of the three inputs we generated a measurement matrix. For identification purposes, and as a result of sensitivity analysis, we reduced the set of 64 measurement variables. We selected five variables, i.e., five outputs or five columns of the measurement matrix. We did this for

[2] MATLAB is a registered trademark of The Math Works, Inc.

each of the three driving points. We also applied one in-plane excitation at 2/3 of the tower height. To see the difference in the frequency response, i.e., to establish that the excitation and consequently the identification of different modes depends on both the driving point and the set of measurement points, we performed the identification twice. We used the set of out-of-plane measurement points the first time and the properly selected set of in-plane measurement points the second time. Corresponding pairs of measurement points, related to measuring acceleration in two different directions, have the same locations on the wind turbine structure.

The important conclusion for modal testing on a real wind turbine structure is that the number of measurement points can be substantially reduced without loss of the modal information. Such a properly selected driving point-measurement set leads to accurate identification. This statement is supported by comparing frequency responses for a given excitation point and different outputs. It can be seen from frequency responses for any driving point that the frequency response for a *collocated excitation-measurement pair* gives the best resolution of the system's resonance modes.

4 WIND TURBINE STATE-SPACE MODEL IDENTIFICATION

The state-space model is generated using a proper input-output sequence, generated as discussed in Section 2 and Section 3. The discrete-time state-space model (A,B,C,D) to be identified, defines the following relation between the scalar driving excitation $u(k)$ and the measurement m-vector (or output) $y(k)$:

$$\begin{aligned} x(k+1) &= Ax(k) + Bu(k) \\ y(k) &= Cx(k) + Du(k) \end{aligned} \tag{5}$$

Note that this state space model depends on the choice of the state vector $x(t)$ and the sampling interval T. Assuming that $x(0)= 0$ and solving for the system output, we obtain

$$y(k) = \sum_{i=1}^{k} CA^{i-1}Bu(k-i) + Du(k) \tag{6}$$

Equation (6) represents the convolution of the system's input sequence $u(k)$ and the sequence $Y(k)$ with the following elements:

$$Y_0 = D,\ Y_1 = CB,\ Y_2 = CAB,\ \ldots,\ Y_k = CA^{k-1}B \tag{7}$$

Therefore, these elements represent consecutive samples of the system's pulse response and are known as Markov parameters. Assuming that our input-output sequence has a length of l, we can write l equations of the type of (6) with the number of terms on the right side increasing as the new input-output pairs become available. This set of l equations can be represented by the following equation:

$$\begin{aligned} &[y(0)\vdots y(1)\vdots \ldots \vdots y(l-1)] = \\ &[D\vdots CB\vdots CAB\vdots \ldots \vdots CA^{l-2}B] \begin{bmatrix} u(0) & u(1) & u(2) & \ldots & u(l-1) \\ & u(0) & u(1) & \ldots & u(l-2) \\ & & u(0) & \ldots & u(l-3) \\ & & & & \vdots \\ & & & & u(0) \end{bmatrix} \end{aligned} \tag{8}$$

The wind turbine structure is a flexible structure with lightly damped low-frequency modes. For such a system and a sufficiently large p,

$$A^k \approx 0 \quad for \quad k \geq p$$

This signifies that to solve for the Markov parameters as an adequate system representation, a sufficiently large l is required.

As alternative possible approach is to artificially increase system damping to solve for Markov parameters. The observer model of the system is used in this approach. The state equation (5) can be manipulated as follows:

$$\begin{aligned} x(k+1) &= Ax(k) + Bu(k) + Gy(k) - Gy(k) \\ &= (A+GC)x(k) + (B+GD)u(k) - Gy(k) \end{aligned} \tag{9}$$

where G is an $n\times m$ matrix chosen to make $A+GC$ as stable as desired. Equation (9) can be rewritten in a standard compact form:

$$x(k+1) = \bar{A}x(k) + \bar{B}v(k) \tag{10}$$

where

$$\bar{A} = A + GC, \quad \bar{B} = [B + GD \quad -G], \quad v(k) = \begin{bmatrix} u(k) \\ y(k) \end{bmatrix}$$

Now, we can write an equation, similar to (8), but one which involves observer Markov parameters:

$$\bar{Y} = \left[D\vdots C\bar{B}\vdots C\bar{A}\bar{B}\vdots \ldots \vdots C\bar{A}^{p-1}\bar{B}\vdots \ldots \vdots C\bar{A}^{l-2}\bar{B}\right] \tag{11}$$

For an observable system, we can assign the eigenvalues of $\bar{A}$ arbitrarily through a proper choice of G. In the case of the dead beat observer, i.e., when all the eigenvalues of $\bar{A}$ are placed at the origin, $C\bar{A}^k\bar{B} \approx 0$ *for* $k \geq p$ where p is a sufficiently large in-

teger. We then solve for the observer Markov parameters

$$\bar{Y} = \left[D : C\bar{B} : C\bar{A}\bar{B} : \ldots : C\bar{A}^{p-1}\bar{B} \right] \qquad (12)$$

using a least-squares algorithm.

The observer Markov parameters in equation (12) include the system Markov parameters and the observer gain Markov parameters. The system Markov parameters are used to compute the system matrices *A*, *B*, *C*, and *D*, whereas the observer gain Markov parameters are used to determine the observer gain matrix G. The proper algorithm for obtaining these Markov parameters has been introduced by Phan et al. [6] and is also discussed by Juang [3]. Software implementation of this identification algorithm was developed at NASA Langley and is known as the Matlab function OKID. Finally, the state-space representation (*A*, *B*, *C*, *D*) of the system is obtained using the Eigensystem Realization Algorithm (ERA), based on system realization theory [3].

It can be proven that the truncated observer model (12), obtained as a result of the dead beat approximation of equation (10), produces the same input-output map as a Kalman filter if the data length is sufficient so that the truncation error is negligible. In this case, *G*, when computed from the combined Markov parameters of equation (12), gives the steady-state Kalman filter gain $K = -G$.

5 IDENTIFICATION PROCEDURE

The identification of the Observer/Kalman Filter model of a wind turbine is performed by the MATLAB program **flokuy.m** which uses the MATLAB function **okid**. The initial estimate of the number of observer Markov parameters is specified considering that the maximum system order that can be identified equals the product $p \bullet m$ where p is the number of Markov parameters considered and m is the number of measurements (or outputs). Using the measurement matrix, the Hankel matrix is formed and a plot of its singular values is displayed to aid in selecting the correct system order. After selecting system order, the percentage of data realized by the model is computed. It is recommended to choose the lowest system order resulting in 100% realization of the measurement data. The corresponding modal parameters are also displayed on the screen in a tabular form showing the mode singular values (SV) and modal amplitude coherence (MAC) factors. This provides additional evaluation of the quality of the identified model. Examining this table, the user can determine the modes whose contribution to the system dynamics is insignificant. Such modes can be classified as the noise modes.

The identified system matrices *A*, *B*, *C*, *D*, generated by the program for the structure model of a selected order, are available as MATLAB variables *Af*, *Bf*, *Cf*, *Df*. The identification error is displayed in the Figure Window.

The next step is to run other identification programs for all input-output data files. They return the list of identified eigenvalues and corresponding modal frequencies in [rad/s] and [Hz], as well as system zeros related to the selected output. The frequency response plot is also displayed in the Figure Window. A special program can be used to enlarge a selected portion of this plot.

All the outlined steps of the above procedure are illustrated in the Appendix, where a case study is presented using simulation data obtained from the ADAMS model of the Micon 65/13 wind turbine.

6 CONCLUSION

The input-output time-series obtained from the virtual wind turbine were used to develop and to validate the identification procedure presented above. It was found that to identify all vibration modes, we have to process, repeating the same procedure, the input/output time-series for both in-plane and out-of-plane excitations applied at various points of the wind-turbine structure. This has been done for three data files generated by out-of-plane excitations, collocated with the measurements near the tips of two blades and at 2/3 of the height of the tower, and for one data file generated by the in-plane excitation collocated with the measurement at 2/3 of the height of the tower.

For each of the four above listed data files, each containing five measurements, the Observer/Kalman Filter state-space model was identified interactively in order to determine the model order providing the best fit for the measurement data. The corresponding set of modal parameters was generated. Then, for each of the five input-output pairs, the frequency response was plotted and the corresponding set of system zeros and their frequencies determined.

The Appendix presents the scope of the tests performed. It also gives the numerical results of modal parameter identification, graphically illustrated by frequency response plots. This graphical illustration is most distinct on the frequency response plot for the system output (measurement) collocated with the excitation used to obtain the analyzed data file.

Examining all the capabilities of the developed identification software tools, it seems that the scope of applied research this software could support is very broad.

7 REFERENCES

[1] Bialasiewicz, J. T. 1994. *Advanced System Identification Techniques for Wind Turbine Structures with Special Emphasis on Modal Parameters*, NREL/TP-442-7110, Golden, CO: National Renewable Energy Laboratory.

[2] James,G.H., III; Carne T.G.; and Lauffer J.P. February 1993. *The Natural Excitation Technique (NExT) for Modal Parameter Extraction from Operating Wind Turbines*, SAND92-1666. Albuquerque, NM: Sandia National Laboratories.

[3] Juang, J.-N. 1994. *Applied System Identification*, Englewood Cliffs, New Jersey, Prentice Hall.

[4] Juang, J.-N.; Horta, L.G.; and Phan M. February 1992. "System/Observer/Controller Identification Toolbox", *NASA Technical Memorandum 107566*, NASA LaRC.

[5] Juang, J.-N.; Phan, M.; Horta, L.G.; and Longman, L.G. 1993. "Identification of Observer and Kalman Filter Markov Parameters: Theory and Experiments," *Journal of Guidance, Control and Dynamics*, vol.16, No. 2, pp.320-329.

[6] Phan, M.; Horta, L.G.; Juang, J.-N.; and Longman, R.W. June 1992."Linear System Identification Via an Asymptotically Stable Observer," *NASA Technical Paper 3164*.

[7] Landau, I.D. 1990. *System Identification and Control Design*, Englewood Cliffs, New Jersey: Prentice Hall.

[8] Newland D.E. 1984. *An Introduction to Random Vibrations and Spectral Analysis*, New York: Longman.

ACKNOWLEDGMENT

The authors would like to thank Marshall Buhl of NREL for providing the input-output data from his ADAMS model of the Micon 65/13 wind turbine system. We appreciate Mr. Buhl's ingenuity and perseverance in adapting the ADAMS code so that the analytical model produced meaningful data for use with the system identification techniques described in this paper.

APPENDIX: A CASE STUDY

This appendix illustrates system identification procedure with special emphasis on identification of modal parameters. ADAMS simulation data for the Micon 65/13 wind turbine is used to illustrate the system identification procedure.

As outlined in Section 3, the excitation of all modes requires obtaining input-output time series for both in-plane and out-of-plane excitations applied at various points of a wind turbine structure. For out-of-plane excitations, collocated with three of the measurements, five measurements listed in Table A-1 have been selected and the corresponding reduced measurement data files have been formed. In addition, one in-plane excitation, collocated with the measurement TOWER4_Y, has been applied. The measurements included in the reduced data file, formed for this excitation, are listed in Table A-2. The measurements included in all these data files are referred in this appendix as outputs with a proper number assigned as shown in Table A-1 and Table A-2.

For all these data files, the same identification procedure was repeated. First, after loading a particular data file into the MATLAB work area, the program that determines the state-space model is executed. The user is asked for the number of outputs (or number of measurements) and the number of Markov parameters to be considered and then decides what the order of the system model to be generated should be. After selecting a particular order, the percentage of data realized by the model is computed. Using a trial and error procedure, the user can find the lowest system order resulting in the 100% realization of the measurement data. The program identifies a state-space representation of a system (in the form of an Observer/Kalman Filter model) and returns the identified system's modal parameters (modal frequencies and damping values) with the corresponding mode singular values and modal amplitude coherence factors. This provides additional evaluation of the quality of the identified model. The identification error is displayed in the Figure Window. Then, the other identification programs are usually repeated a number of times equal to the number of measurement points in the processed data file (five times in the identification process presented below). This is justified by the fact that for each input-output relation in a given file we have the same poles or modal frequencies but different zeros. Therefore, each input-output pair has a different frequency response. As we can see from the identification results presented below, the visibility of the modal frequencies on the frequency response plots is different for different input-output pairs and of course much sharper for those pairs that are collocated. Also, we can observe that for the excitation inputs, applied at any point on the turbine axis of symmetry, the frequency responses for symmetrical outputs are identical. Considering the possible wide range of research avenues which can be pursued using this software, one of the identification programs returns the following list of the identified system parameters: system eigenvalues, modal frequencies, and system zeros and their frequencies.

The numerical and graphical illustration of the identification results is given below using one of the reduced data files and plotting the frequency response for a

collocated input-output pair. The 34th order model has been identified The identification error is shown in Fig. A-1. The identified system eigenvalues are listed in Table A-3 with the corresponding modal frequencies listed in Table A-4. The identified system zeros, associated with the collocated input-output pair, are listed in Table A-5 with the corresponding frequencies listed in Table A-6. Finally, the frequency response is shown in Fig. A-2 on a logarithmic scale and for the full frequency range, and in Fig. A-3 on a linear scale, obtained for a frequency range of interest using a zooming program.

Table A-1 Out-of-plane measurements

TOWER4_Z	or column 12	OUTPUT 1
SLRING_Z	or column 15	OUTPUT 2
B1S13_Y	or column 24	OUTPUT 3
B2S13_Y	or column 32	OUTPUT 4
B3S13_Y	or column 40	OUTPUT 5

Table A-2 In-plane measurements

TOWER4_Y	or column 4	OUTPUT 1
SLRING_Y	or column 7	OUTPUT 2
B1S13_Z	or column 48	OUTPUT 3
B2S13_Z	or column 56	OUTPUT 4
B3S13_Z	or column 64	OUTPUT 5

Table A-3 Identified system eigenvalues

r1 =
-1.3346e+001+ 2.7233e+002i
-1.3346e+001- 2.7233e+002i
-1.8295e+001+ 2.5914e+002i
-1.8295e+001- 2.5914e+002i
-9.6893e+000+ 2.1843e+002i
-9.6893e+000- 2.1843e+002i
-1.1474e+001+ 2.0598e+002i
-1.1474e+001- 2.0598e+002i
-1.0435e+001+ 1.8812e+002i
-1.0435e+001- 1.8812e+002i
-1.5566e+002
-7.5905e+000+ 1.2766e+002i
-7.5905e+000- 1.2766e+002i
-1.2341e+001+ 1.1345e+002i
-1.2341e+001- 1.1345e+002i
-5.8522e+000+ 9.9550e+001i
-5.8522e+000- 9.9550e+001i
-5.9147e+001
-5.4268e+000+ 7.7330e+001i
-5.4268e+000- 7.7330e+001i
-1.3009e+001+ 7.2863e+001i
-1.3009e+001- 7.2863e+001i
-3.6530e+000+ 6.7912e+001i
-3.6530e+000- 6.7912e+001i
-3.4150e+000+ 5.4387e+001i
-3.4150e+000- 5.4387e+001i
-1.0776e+001+ 4.3325e+001i
-1.0776e+001- 4.3325e+001i
-1.3177e+000+ 2.1992e+001i
-1.3177e+000- 2.1992e+001i
-5.0585e-001+ 2.0080e+001i
-5.0585e-001- 2.0080e+001i
-1.0685e+000+ 1.1023e+001i
-1.0685e+000- 1.1023e+001i

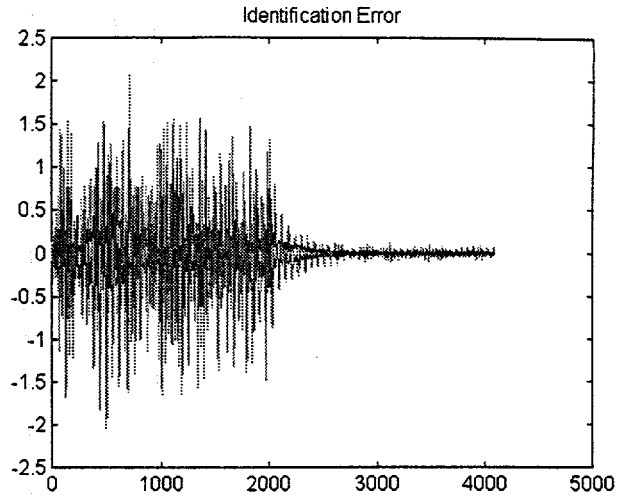

Fig. A-1 Identification error as function of the number of measurement points

Table A-4 Identified modal frequencies

rad/s	Hz
fr =	
2.7266e+002	4.3395e+001
2.7266e+002	4.3395e+001
2.5978e+002	4.1346e+001
2.5978e+002	4.1346e+001
2.1865e+002	3.4799e+001
2.1865e+002	3.4799e+001
2.0630e+002	3.2834e+001
2.0630e+002	3.2834e+001
1.8841e+002	2.9987e+001
1.8841e+002	2.9987e+001
1.5566e+002	2.4774e+001
1.2789e+002	2.0354e+001
1.2789e+002	2.0354e+001
1.1412e+002	1.8163e+001
1.1412e+002	1.8163e+001
9.9722e+001	1.5871e+001
9.9722e+001	1.5871e+001
5.9147e+001	9.4135e+000
7.7520e+001	1.2338e+001
7.7520e+001	1.2338e+001
7.4015e+001	1.1780e+001
7.4015e+001	1.1780e+001
6.8010e+001	1.0824e+001
6.8010e+001	1.0824e+001
5.4494e+001	8.6730e+000
5.4494e+001	8.6730e+000
4.4645e+001	7.1055e+000
4.4645e+001	7.1055e+000
2.2031e+001	3.5064e+000
2.2031e+001	3.5064e+000
2.0086e+001	3.1968e+000
2.0086e+001	3.1968e+000
1.1075e+001	1.7626e+000
1.1075e+001	1.7626e+000

Table A-5 Identified system zeros related to the OUTPUT 1

```
ZER =
 3.1139e+002+ 3.6853e+002i
 3.1139e+002- 3.6853e+002i
-2.1704e+001+ 2.5902e+002i
-2.1704e+001- 2.5902e+002i
-1.0073e+001+ 2.3527e+002i
-1.0073e+001- 2.3527e+002i
-1.5076e+001+ 2.1052e+002i
-1.5076e+001- 2.1052e+002i
-2.4163e+001+ 1.9487e+002i
-2.4163e+001- 1.9487e+002i
-1.9364e+001+ 1.3254e+002i
-1.9364e+001- 1.3254e+002i
-4.8435e+000+ 1.0962e+002i
-4.8435e+000- 1.0962e+002i
 3.3462e+001+ 9.5703e+001i
 3.3462e+001- 9.5703e+001i
-8.0594e+001
-9.1650e+000+ 8.4268e+001i
-9.1650e+000- 8.4268e+001i
-4.3114e+000+ 7.0832e+001i
-4.3114e+000- 7.0832e+001i
-8.1020e+000+ 6.5483e+001i
-8.1020e+000- 6.5483e+001i
-1.7053e+001+ 4.8927e+001i
-1.7053e+001- 4.8927e+001i
-3.4549e+000+ 5.0486e+001i
-3.4549e+000- 5.0486e+001i
-9.2851e+000+ 1.6901e+001i
-9.2851e+000- 1.6901e+001i
-3.1281e+000+ 2.0829e+001i
-3.1281e+000- 2.0829e+001i
-3.7882e-001+ 1.9711e+001i
-3.7882e-001- 1.9711e+001i
 4.0870e+000
```

Table A-6 Identified zero frequencies

```
        rad/s          Hz
zfr =
  4.8247e+002   7.6788e+001
  4.8247e+002   7.6788e+001
  2.5992e+002   4.1368e+001
  2.5992e+002   4.1368e+001
  2.3548e+002   3.7478e+001
  2.3548e+002   3.7478e+001
  2.1106e+002   3.3591e+001
  2.1106e+002   3.3591e+001
  1.9636e+002   3.1252e+001
  1.9636e+002   3.1252e+001
  1.3395e+002   2.1318e+001
  1.3395e+002   2.1318e+001
  1.0972e+002   1.7463e+001
  1.0972e+002   1.7463e+001
  1.0138e+002   1.6136e+001
  1.0138e+002   1.6136e+001
  8.0594e+001   1.2827e+001
  8.4765e+001   1.3491e+001
  8.4765e+001   1.3491e+001
  7.0963e+001   1.1294e+001
  7.0963e+001   1.1294e+001
  6.5982e+001   1.0501e+001
  6.5982e+001   1.0501e+001
  5.1813e+001   8.2464e+000
  5.1813e+001   8.2464e+000
  5.0604e+001   8.0539e+000
  5.0604e+001   8.0539e+000
  1.9283e+001   3.0690e+000
  1.9283e+001   3.0690e+000
  2.1063e+001   3.3522e+000
  2.1063e+001   3.3522e+000
  1.9715e+001   3.1377e+000
  1.9715e+001   3.1377e+000
  4.0870e+000   6.5047e-001
```

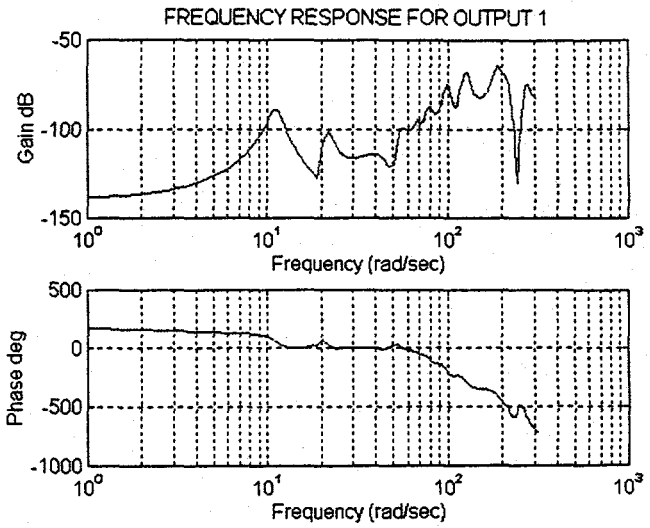

Fig. A-2 Frequency response for a collocated input-output pair.

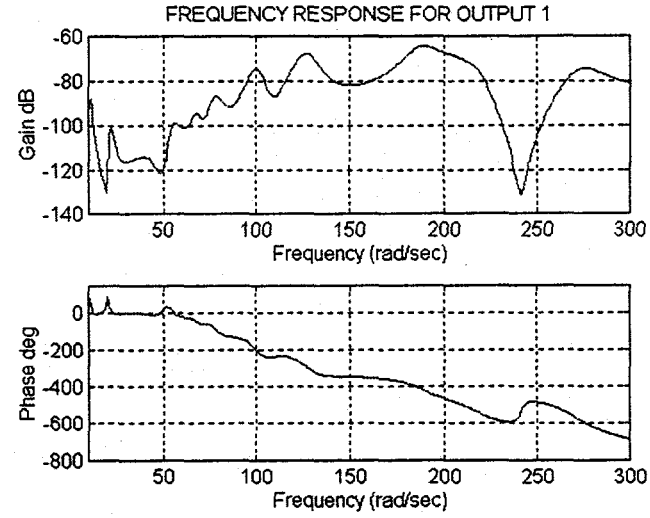

Fig. A-3 Frequency response of Fig. A-2 shown on a linear scale in the frequency range of interest.